Research on Biomedical Engineering
https://doi.org/10.1007/s42600-020-00102-7

ORIGINAL ARTICLE

Effects of photobiomodulation associated with chitosan viscosupplementation for osteoarthritis: an in vitro and in vivo study

Carla Roberta Tim[1,2] · Cintia Cristina Santi Martignago[3] · Livia Assis[1,2] · Ana Laura Andrade[3] · Lia Mara Neves[4] · Cynthia Castro[5] · Nivaldo Parizotto[1] · Juliana Carolina Tarocco[1] · Richard Liebano[3] · Márcia Cominetti[6] · Karina Nogueira Zambone Pinto[5] · Ana Claudia Muniz Rennó[2]

Received: 10 February 2020 / Accepted: 28 September 2020

Abstract

Purpose The aim of the present study was to investigate the tissue performance of the association of photobiomodulation (PBM) and chitosan hydrogel (Ch), using in vitro and in vivo studies, in culture of chondrocytes and in an experimental model of osteoarthritis (OA) in the knee of rats.

Methods The chitosan hydrogel was characterized by pH, gelation time, and degradation rate. For the in vitro study, chondrocyte cells were seeded in the Ch irradiated or not with PBM to assess cell viability and proliferation after 1, 3, and 5 days. For the in vivo study, sixty Wistar rats with OA were randomly distributed: control group (CG), Ch hydrogel injection (Ch), Ch hydrogel injection associated with PBM (Ch/PBM).

Results The characterization results revealed that Ch hydrogels can be controlled precisely by variation of the urea and urease concentrations. The in vitro findings demonstrated that Ch and Ch/PBM are biocompatible and noncytotoxic. The in vivo findings showed that PBM associated with Ch prevented articular degeneration by stimulating anabolic factor (TGF-β) and reducing catabolic factor (TNF-α) and increasing the gene related to components of the cartilage extracellular matrix.

Conclusion In conclusion, the PBM associated with Ch can be used as a cartilage repair application.

Keywords Photobiomodulation · Articular cartilage · Knee osteoarthritis · Chitosan · Viscosupplementation

Introduction

Osteoarthritis (OA) is a multi-causal joint disease, which leads to progressive degeneration of the articular cartilage, subchondral bone remodeling and fibrillation, and inflammation of the periarticular soft tissues such as joint ligaments, capsule, synovial membrane, and muscles, culminating in a full thickness loss of the joint surface (Rieger et al. 2017). Consequently of all the morphological modifications, a series of functional deficits are observed such as the decrease of muscle strength, impairment in balance and proprioception, increasing risk of falls and the level of (Levinger et al. 2011; Roos et al. 2011).

Therefore, the development of innovative and more efficient therapeutical intervention to treat OA symptoms is of extreme clinical importance (Comblain et al. 2017). In this context, photobiomodulation (PBM), also known as low-level laser therapy, has also been considered a very promising therapeutic intervention for cartilage tissue engineering, mainly due to its stimulatory effect on tissue metabolism and ability of modulating the inflammatory process after an injury (Bjordal et al. 2010; Hamblin 2016). Several studies have demonstrated, in experimental models of joint inflammation, that PBM can decrease the expression of chemotactic factors and inflammatory cytokines and increase antioxidant enzyme

✉ Carla Roberta Tim
carlinha_tim@hotmail.com

1 Department of Biomedical Engineering, Institute of Science and Technology of Brasil University, Carolina Fonseca, 235, São Paulo, SP, Brazil

2 Department of Bioscience, Federal University of São Paulo, Santos, SP, Brazil

3 Department of Physiotherapy, Federal University of São Carlos, São Carlos, SP, Brazil

4 Department of Physiology, Federal University of São Carlos, São Carlos, SP, Brazil

5 Departments of Morphology and Pathology, Federal University of São Carlos, São Carlos, SP, Brazil

6 Departments of gerontology, Federal University of São Carlos, São Carlos, SP, Brazil

Published online: 01 October 2020

levels (Bublitz et al. 2014; Pallotta et al. 2012). Also, clinical trials have been demonstrated that PBM is able of reducing pain levels, articular stiffness, and swelling, increasing the functional performance in patients with OA (Rayegani et al. 2012; Yurtkuran et al. 2007).

Similarly, biomaterials for articular viscosupplementation such as hyaluronic acid (HA) and chitosan (Ch) have been frequently used (Comblain et al. 2017). Chitosan is a cationic polysaccharide which is derived from naturally chitin and it has gained lots of attention due to its ability to stimulate tissue repair (Yan et al. 2014a), anti-inflammatory effects (Chung et al. 2012), and biocompatibility (Vandevord et al. 2002). Chitosan has a number of commercial and possible biomedical applications, such as bandages to reduce bleeding, antibacterial effects, and articular viscosupplementation (Comblain et al. 2017; Dantas et al. 2011). Recently, in vitro studies have suggested that chitosan could induce the expression of cartilage matrix components (such as collagen and proteoglycans) and reduce inflammatory and catabolic mediator's production by chondrocytes (Comblain et al. 2017; Dantas et al. 2011). Furthermore, in vivo studies demonstrated that Ch prevented cartilage degradation and synovial membrane inflammation in experimental models of OA (Kaderli et al. 2015; Zhang et al. 2017).

Although, there are many evidence that PBM and Ch have positive stimulatory effects on joints with OA, the effects of the association of both treatments were not studied yet. In this context, based on the promising effects of PBM and Ch on OA, it was hypothesized that both therapeutic approaches, used in association, may favor the metabolism of chondrocytes (using in vitro studies) in the cartilage structure and, also, decrease the inflammatory process in an experimental model of OA. Thus, the aim of the present study was to investigate the tissue performance of the association of photobiomodulation and chitosan hydrogel, using in vitro and in vivo studies, in culture of chondrocyte cells and in an experimental model of OA in the knee of rats, respectively. For this, we developed a first study where the more appropriated protocol for Ch hydrogel manufacturing was developed and the characterization of the samples was made. After that, the chosen samples were used for the biological studies.

Materials and methods

Preparation of chitosan hydrogels

Chitosan (Sigma-Aldrich, St. Louis, MO, USA) was dissolved at a concentration of 2.5 w/v% in 0.100 M HCl. Urease (type III from Jack beans, U1500, Sigma-Aldrich, St. Louis, MO, USA) was dissolved in sterile phosphate-buffered saline, (PBS, pH 7.4) at a concentration of 30 and 50 U mL. Urea (Sigma-Aldrich, St. Louis, MO, USA) was dissolved at a concentration of 7.5 and 10 M in Milli-Q (Millipore, Burlington, MA, EUA) water and sterilized by filtration over a 0.2-μm filter.

In order to prepare 1.5 w/v% chitosan hydrogels, 1 mL chitosan solution was mixed with 0.67 mL urease (30 or 50 U mL), according to a previous study (Yan et al. 2014b). Thereafter, 10 μL of the urea (7.5 or 10 M) solution was added and mixed at room temperature which resulted into hydrogel solutions (Table 1). For the hydrogel used in the degradation test and in vitro experiments, the chitosan was mixed with urease and urea, and then the hydrogel was injected into Teflon molds (4 mm in diameter and 3-mm thick). After gelation time at room temperature, hydrogels were removed from the molds.

Characterization of the chitosan hydrogel

pH versus time

The pH analysis was performed with the pH meter electrode (Kasvi, Paraná, Brazil) placed in a hydrogel freshly prepared immediately after addition of the 10 μL urea. Thus, the pH was recorded for 1, 3, 10, and 45 min at room temperature. The pH was recorded to investigate the speed at which the pH changed under different hydrogel compositions (Yan et al. 2014b).

Optimization of the gelation kinetics

The inverted vial method was used to assessed gelation time, as described by Wang et al. (2017). Briefly, 1 mL of freshly prepared hydrogel solution was placed in a 2-mL Eppendorf vial. To determine the gel transition time, the vials were inverted horizontally every 30 s and the time at which the hydrogel did not flow was recorded as the gelation time.

Degradation rate

The degradation of the chitosan hydrogel in buffer solutions was determined by mass loss. Hydrogels were incubated in 10 mL of PBS containing 1.5 μg/mL lysozyme (Sigma-Aldrich, St. Louis, MO, USA) at 37 °C. The medium was

Table 1 Different formulations of the chitosan hydrogel

Groups	Urease (U/mL)	Urea (M)
30 U/7.5 M	30	7.5
50 U/7.5 M	50	7.5
30 U/10 M	30	10
50 U/10 M	50	10

refreshed every 3 days and the mass of the (patted-dry) hydrogels was monitored at 15, 30, and 60 days. The degradation rate was expressed as the percentage of the remaining weight (initial weight − final weight) (Chen et al. 2014).

In vitro experiments

Procedures for chondrocyte extraction

All the experiments involving animals were approved by the Institutional Animal Care Committee guidelines (2478130315).

For chondrocyte extraction, three Wistar rats (weight ± 100 g) were anesthetized with ketamine chloride (80 mg/kg) (Syntec, São Paulo, Brazil) and xylazine (10 mg/kg) Syntec, São Paulo, Brazil), and cartilage samples from both femurs were removed using a scalpel. Immediately after the surgery, the animals were euthanized individually by carbon dioxide asphyxia.

Slices of cartilage were incubated in 0.25% type I collagenase in Dulbecco's modified Eagle's medium (DMEM) (Vitrocell, Brazil), overnight at 37 °C in 5% CO_2. The cells were then seeded onto tissue culture flasks for expansion and maintained as subconfluent monolayers in DMEM. Cells from the 4th passage were used for the in vitro experiments.

All the procedures were performed under strict aseptic conditions in a biological safety cabinet. For the in vitro experiments, cells were divided into 3 groups: (1) control group (CG): cells seeded on tissue culture plastic, (2) chitosan group (Ch): cells seeded on chitosan 30 U/mL urease and 10 M urea, (3) chitosan and PBM group (Ch/PBM): cells seeded on chitosan 30 U/mL urease and 10 M urea and irradiated with PBM 1.4 J.

Prior to cell seeding, chitosan hydrogel solution containing urea (10 M) and urease (30 mL) dissolved in culture medium was placed in 35-mm Petri plate and incubated in tissue culture growth medium supplemented with 10% FBS (Life Technologies, Carlsbad, USA) at 37 °C, and 5% CO_2 for at least 24 h, in order to remove possible side products of the hydrogel formation (such as NH3). After this period, the medium was discarded. Subsequently, chondrocytes were seeded in direct contact with the chitosan hydrogen at a density of 5.10^4 cells/0.75 cm^2. The cell culture medium was changed every 2–3 days, and the cells were cultured for 1, 3, and 5 days.

PBM by gallium-aluminum-arsenide (GaAlAs) diode (Photon Laser II, DMC® equipment Ltda, SP, São Carlos, Brazil) was used in the following parameters: 808-nm wavelength, continuous irradiation mode, 0.028-cm^2 spot area, energy density 50 J/cm^2, 50-mW power output, 28-s irradiation time, 1.4-J total energy. The PBM irradiation was performed with the laser pointer tip in direct contact with the plate every 24 h. One, three, or 5 days after irradiation, cell viability and proliferation were assessed.

Determination of cell metabolic activity

Alamar Blue® (Thermo Fisher Scientific, Waltham, MA, EUA) was used to evaluate cell metabolic activity. Alamar Blue® was diluted in cell culture media (10%), and it was added directly to chondrocytes. Following, the plate was incubated in a cell culture incubator at 37 °C for 4 h. Afterwards, 200 μL of each sample was transferred to a 96-well plate (in duplicates). Finally, the plate was read in a spectrophotometer (Bio-Tek Instruments, Winooski, USA) at 570 nm and 600 nm (van Houdt et al. 2015).

Cell proliferation

In order to determine, cell proliferation was quantified the amount of DNA by using the Quanti Fluor® dsDNA quantitation kit (Promega, Leiden, The Netherlands). After the cell culture experiments, chondrocytes were washed with PBS twice, homogenized in 1 mL of Milli-Q water, frozen, and thawed twice before analysis. Subsequently, 100 μL of the DNA sample or standard was incubated with 100 μL of working solution in the dark for 10 min. Then, the samples were read in a spectrophotometer (Bio-Tek Instruments, Winooski, USA) at 530 nm (van Houdt et al. 2015).

In vivo experiments

Surgical procedures

Good laboratory animal practice was observed according to the international standards for animal experimentation and following approval by our institution's Animal Care and Ethics Committee (2478130315). Animals were maintained in plastic cages with sawdust bedding, with light–dark periods of 12 h and controlled temperature (24 ± 2 °C), and with unrestricted access to water and commercial diet.

All animals were submitted to general anesthesia induced by intraperitoneal injection of 80 mg/kg ketamine (Dopalen; Vetbrands; São Paulo; Brazil) and 10 mg/kg xylazine (Anasedan; Vetbrands; São Paulo; Brazil). The left knee was trichotomized and sterilized, then a skin incision lateral parapatellar was carried out, whereby the patella was dislocated laterally to provide access to the joint space. After, with the flexed knee, the anterior cruciate ligament (ACL) was isolated and transected. The complete transection of the ligament was confirmed by Lachman testing. Thus, incision was sutured and antiseptically treated. Furthermore, all rats were given appropriate postoperative care. The knee OA induction protocol was performed as previously described by Galois et al. (2004). Animals were randomly divided into 3 groups (n =

20 per group): (1) CG: OA animals without treatment, (2) Ch: OA animals submitted to chitosan hydrogel injection, (3) Ch/PBM: OA animals submitted to chitosan hydrogel injection and PBM.

Treatment

Chitosan hydrogels were prepared as described above. According to our characterization results, chitosan hydrogel containing 10 m urea and 30 U/mL urease was used based on its handling properties. Then, the chitosan hydrogel (30 μL) was injected intra-articular 4 weeks after knee OA induction.

PBM treatment with GaAlAs diode (Photon Laser II, DMC® equipment Ltda, SP, São Carlos, Brazil) started 4 weeks after OA induction. For the treatment, PBM was used in the following parameters: 808-nm wavelength, continuous irradiation mode, 0.028-cm^2 spot area, energy density 50 J/cm^2, 50-mW power output, energy 1.4 J, and 28-s irradiation time. PBM was applied through the punctual contact technique at 2 points on medial and lateral sides of knee joint, 3 days/week, for 12 and 24 sessions (4 and 8 weeks of treatment, respectively).

Retrieval of specimens

Rats were individually euthanized by carbon dioxide asphyxia in different set points (4 and 8 weeks after treatments). Then, left knees were removed and immediately fixed in 10% formaldehyde (Merck, Darmstadt, Germany) for 24 h.

After fixed, the specimens were decalcified in 4% diamine tetra-acetic acid (EDTA) (Merck, Darmstadt, Germany) and embedded in paraffin blocks. Thin sections (5 μm) were prepared in the longitudinal plane, using a micrometer (Leica RM-2145, Wetzlar, Germany). Afterwards, the laminas were stained with hematoxylin and eosin (HE stain, Merck, Darmstadt, Germany). Moreover, other sections were obtained for the immunohistochemical analysis.

Histological descriptive analysis

The samples stained with HE were used to evaluate histopathological alterations in the articular cartilage. Thus, two blinded observers performed the descriptive analysis assessing cellular organization, cartilage structure, and amount of cells. The specimens were examined using a light microscope (× 100; Leica Microsystems AG, Wetzlar, Germany) (Sanches et al. 2018).

OARSI score system

The progression of OA was assessed and compared according to the Osteoarthritis Research Society International (OARSI). Two experienced observers performed the scoring in a blinded manner. Briefly, the system evaluated for the presence of osteoarthritis grade (OARSI grades 0 to 6) and osteoarthritis stage (OA stages 0 to 4). Thus, it results in the osteoarthritis scoring (OA scoring: (OARSI grade) × (OA stage)) (Sanches et al. 2018).

Immunohistochemistry analysis

For the immunohistochemistry analysis, the sections were deparaffinized and rehydrated in graded ethanol; each specimen was pretreated in a steamer (Philips Walita, Brazil) with 0.01 M citric acid buffer (pH 6) for 5 min for antigen retrieval. After, the endogenous peroxidase was inactivated with 0.3% hydrogen peroxide in PBS solution for 20 min and then blocked with 5% normal goat serum in PBS solution for 10 min. Following, the specimens were incubated with anti-IL4 polyclonal primary antibody at a concentration of 1:200 (Santa Cruz Biotechnology, Santa Cruz, USA) overnight at 4 °C in a refrigerated environment. This was followed by application of biotin-labeled secondary antibody (ABC kit, PK-6200, Vector laboratories, Burlingame, CA, USA) at 1:5 dilution for 30 min. Colorimetric detection was done with a diaminobenzidine substrate (DAB, SK-4100, Vector laboratories, Burlingame, CA, USA) and hematoxylin (Merck, Darmstadt, Germany). For a negative control, the primary antibody was omitted, and PBS alone was applied.

The immunostaining was assessed according to the presence of the immunomarkers qualitatively and semi-quantitatively in five pre-determined fields using a scoring scale ranging from 1 to 4 (1 = absent, 2 = slight, 3 = moderate, and 4 = intense) for immunohistochemical analysis. The analysis was performed by observers in a blinded manner.

ELISA assays for synovial fluid analyses

In order to obtain the synovial fluid, the cavity was lavage with 0.1 mL saline, and 0.1 mL synovial fluid was aspirated and centrifuged for 10 min at 4500 rpm. Then, the supernatant was stored in Eppendorf tubes at − 80 °C. Concentrations of tumor necrosis factor-α (TNF-α) in synovial fluid samples were measured using the rat TNF-α ELISA Kit (R&D Systems, Minneapolis, USA), following the manufacturer's recommendations. Reactions were read (Bio-Tek Instruments, Winooski, USA) at 450 nm and expressed in pg/mL.

Quantitative real-time polymerase chain reaction

TRIzol reagent (Invitrogen, Carlsbad, CA, USA) was used to isolate total RNA from the cells. In brief, TRIzol reagent was added to the sample and then chloroform was

mixed vigorously with the sample and centrifuged at 12,000*g* for 15 min at 4 °C. Following, the aqueous phase of the sample was collected and mixed with isopropanol and centrifuged. After, the extract was washed with 75% ethanol. Successively, the RNA pellet was dissolved in RNase-free water, and concentration and purity were determined using Nanoview (Life Technologies, Carlsbad, USA). RNA samples with an A260/A280 ratio < 1.8 were excluded.

Total RNA was reverse-transcribed into cDNA, and then the cDNA samples were subjected to quantitative real-time polymerase chain reaction (qRT-PCR) using the Applied Biosystems StepOne™ Real-Time PCR System (Life Technologies, Carlsbad, USA). Oligonucleotide primers were designed for βactin, Collagen 2, and TGF-β (Table 2) using the Primer Express Software 2.0 (Applied Biosystems, Foster City, USA). All real-time primers were initially tested against standards, and a standard curve was generated.

The PCR conditions were 10 min of denaturation at 94 °C, followed by 40 cycles consisting 15 s of denaturation at 94 °C, 1 min of annealing at 60 °C, and 45 s of extension at 72 °C, with a final extension step at 72 °C for 2 min. In addition, negative control reactions with no template (deionized water) were included in each run. The housekeeping gene used to normalize expression data was βactin. The 2-ΔΔCT method was used for the analysis of relative gene expression.

Statistical analysis

The normality of all variable's distribution was verified using Shapiro–Wilk's W test and homogeneity with Levene. The analyses pH versus time, degradation rate, cell proliferation, OARSI score system, ELISA assays for synovial fluid, and quantitative real-time polymerase chain reaction (COL-2 and TGF-β) were data with homogeneous and normal distribution, thus one-way ANOVA was used with the Tukey test. However, the optimization of the gelation kinetics, determination of cell metabolic activity, and immunohistochemistry analysis exhibited non-normal and non-homogeneous data. Thereby, it was performed ANOVA and the Kruskal–Wallis test with the Mann–Whitney post-test. The GraphPad Software (PRISM; La Jolla, CA, USA) was used to carry out the statistics analysis. Values of $p < 0.05$ were considered statistically significant.

Results

Characterization of the chitosan hydrogel

For pH versus time analysis, 1 min after measurement, a significantly lower value was observed in hydrogel 30 U mL/10 M compared with 30 U mL/7.5 M, 50 U mL/7.5 M, and 50 U mL/10 M. Additionally, the 30 U mL/7.5 M showed a lower pH value compared with 50 U mL/7.5 M and 50 U mL/10 M. In the second period analyzed (after 3 min), 30 U mL/7.5 M continued with significantly lower pH values when compared with 50 U mL/7.5 M and 50 U mL/10 M. Similarly, 30 U mL/10 M demonstrated lower statistically significant difference compared with 50 U mL/7.5 M and 50 U mL/10 M. Additionally, in the same period, hydrogel 50 U mL/10 M demonstrated higher values of pH compared with 50 U mL/7.5 M. For 10 min after measurement, it was possible to verify that hydrogel 50 U mL/7.5 M exhibit pH significantly higher compared with 30 U mL/10 M. However, when this hydrogel was compared with 50 U mL/10 M, the results showed a difference significantly lower of pH value for 50 U mL/7.5 M. For the last period, hydrogel 50 U mL/10 M continued with higher pH compared with 30 U mL/7.5 M and 50 U mL/7.5 M. Interesting, hydrogel 50 U mL/7.5 M demonstrated lower statistically significant difference compared with 30 U mL/10 M. The final pH values were controlled by the amount of urea with the highest pH values observed for hydrogel containing the highest urea concentrations (Fig. 1a).

Figure 1b demonstrates the evaluation of the gelation time. Values found for hydrogels containing 30 U/mL urease and 7.5 M urea were significantly higher compared with the values for the other concentrations. Furthermore, hydrogels containing 50 U/mL urease and 10 M urea presented a statistically smaller concentration when compared with other concentrations.

The percentage of remaining weight after 15, 30, and 60 days mainly depended on the urease concentration, with degradation increasing with increasing urease concentration. Hydrogel containing 50 U/mL urease and 10 M urea demonstrated a higher increase in the degradation rate when compared with hydrogel containing 30 U mL/7.5 M and hydrogel 30 U mL/10 M, after 15 days. In addition, hydrogel 50 U/mL urease and 7.5 M urea presented a higher degradation rate compared with hydrogels containing 30 U mL/7.5 M and hydrogel 30 U mL/10 M, after 60 days (Fig. 1c).

Table 2 Real-time PCR primers

Gene	Forward primer	Reverse primer
βactin	ACCAGTTCGCCATGGATGAC	TGCCGGAGCCGTTGTC
Col-2	CCTTCCCATTGTTGACATTGC	TCCACACCAAATTCCTGATCAG
TGF-β	AAGTGGAATGGGTCGGAAATT	TGAAGGGTGTTCCAAAAACTGA

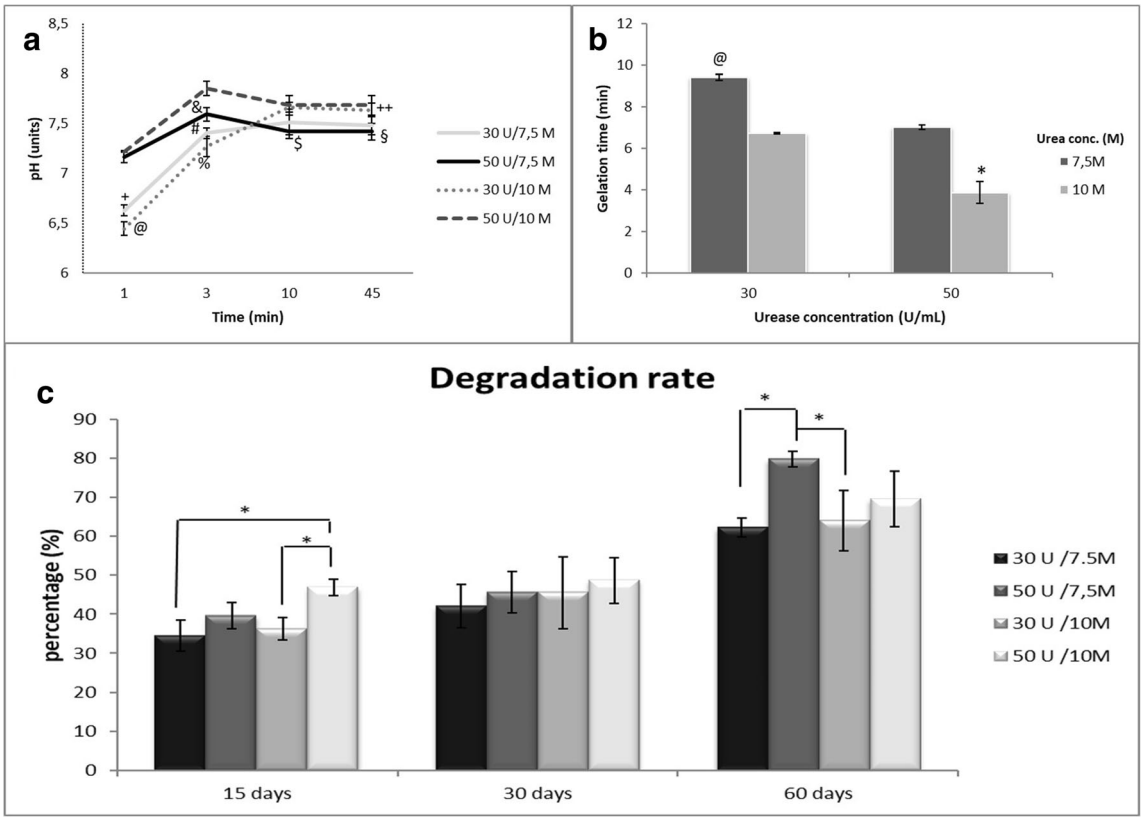

Fig. 1 Characterization of the chitosan hydrogel. **a** pH as a function of urease and urea concentration. **b** Gelation time (min) as a function of urease and urea concentration. **c** Degradation curves for the various hydrogels after soaking for 15, 30, and 60 days in PBS containing 1.5 μg/mL^{-1} lysozyme. Significant differences of $p < 0.05$ are represented by single asterisk (*) and @ versus 30 U mL/7.5 M, 50 U mL/7.5 M, and 50 U mL/10 M. + versus 50 U mL/7.5 M and 50 U mL/10 M. # versus 50 U mL/7.5 M and 50 U mL/10 M. & versus 50 U mL/7.5 M. % versus 50 U mL/7.5 M and 50 U mL/10 M. $ versus 30 U mL/10 M and 50 U mL/10 M; ++ versus 30 U mL/7.5 M and 50 U mL/7.5 M; § versus 30 U mL/10 M. € versus 30 U mL/7.5 M and 30 U mL/10 M. ∞ versus 30 U mL/7.5 M and 30 U mL/10 M

In vitro experiments

Determination of cell metabolic activity

Figure 2a shows the metabolic activity of rat chondrocytes. On days 1, 3, and 5, the cell metabolic activity was significantly higher for CG compared with Ch and Ch/PBM. Interestingly, Ch/PBM was significantly increased compared with Ch only on day 1.

Cell proliferation

Cell proliferation for the chondrocytes is shown in Fig. 2b. For cell proliferation, CG showed significantly lower DNA content values compared with Ch and Ch/PBM on day 1. Interestingly, after 3 days, it was possible to observe a significantly increase DNA content values in CG when compared with Ch and Ch/PBM. At the same period, Ch/PBM showed a significant increase in DNA content values compared with Ch. After 5 days, CG presented a statistically significant increase DNA content values compared with Ch/PBM.

Animal experiment

Histological descriptive analysis

Figure 3a demonstrates an overview of the histopathological analysis of the cartilage tissue for the experimental groups. In the first experimental period, all treated groups presented similar histological findings, with moderate sings of degradation, vertical fissures extending into the mid zone, and hypercellularity of the chondrocytes most prominently adjacent to fissures.

After 8 weeks, histopathologic evaluation exhibited intense signs of degradation, with superficial zone delamination of the entire cartilage surface, clustering of chondrocytes, and cyst formation within the cartilage matrix in CG. Similar, sections from Ch presented fissures and fibrillation along the entire cartilage, abnormal chondrocyte orientation, and proliferation along the superficial layer. However, for Ch/PBM, it presented less intense sings of tissue degradation with initial surface discontinuity at the superficial zone and disorganization of the chondrocytes in the cartilage region when compared with CG.

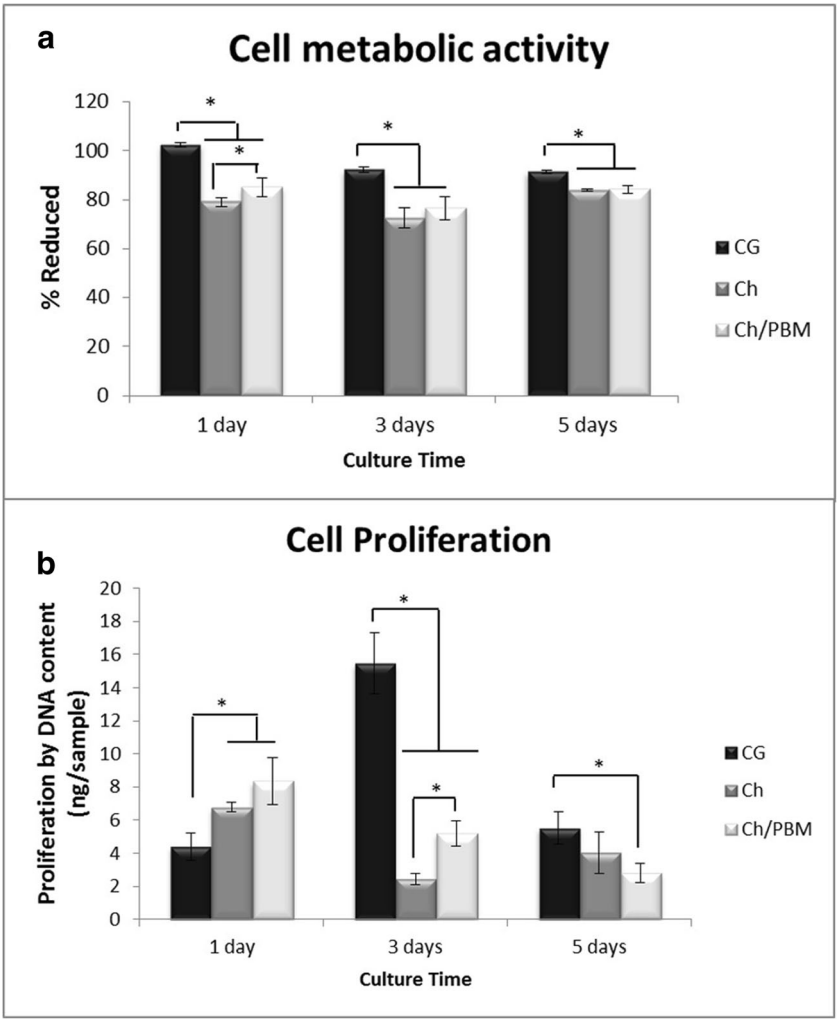

Fig. 2 In vitro experiments. **a** Cell metabolic activity. **b** Cell proliferation by DNA content values. Significant differences of $p < 0.05$ are represented by a single asterisk (*). CG, control group; Ch, chitosan group; Ch/PBM, chitosan and PBM group

OARSI score system

Figure 3b shows the OARSI evaluation for cartilage degeneration. No statistically significant differences were detected among the experimental groups after 4 weeks. In addition, the OARSI score for cartilage degeneration showed a significantly higher score for CG when compared with Ch/PBM, after 8 weeks.

Immunohistochemistry analysis

Qualitative evaluation demonstrated that IL-4 immunostaining was observed mainly in the nucleus of the chondrocytes for all experimental groups (Fig. 4a).

In the first experimental period, semi-quantitative analysis demonstrated no statistically significant differences detected among the groups. Additionally, immunohistochemistry semi-quantitative analysis showed significantly lower IL-4 expression for CG compared with Ch after 8 weeks of treatment. No other difference was observed between the treated groups (Fig. 4b).

ELISA assays for synovial fluid analyses

TNF-α concentration in synovial fluid was markedly increased in all groups. A significant decrease in TNF-α concentration was evident in Ch and Ch/PBM compared with CG after 4 weeks. However, no significant difference was found in the TNF-α after 8 weeks (Fig. 5).

Quantitative real-time polymerase chain reaction

COL-2 gene expression

Figure 6a shows the results of gene expression of COL-2. No significant difference was found among the experimental groups after 4 weeks. In addition, the gene expression analysis exhibited a significant increase of COL-2 observed in the Ch compared with the CG and Ch/PBM.

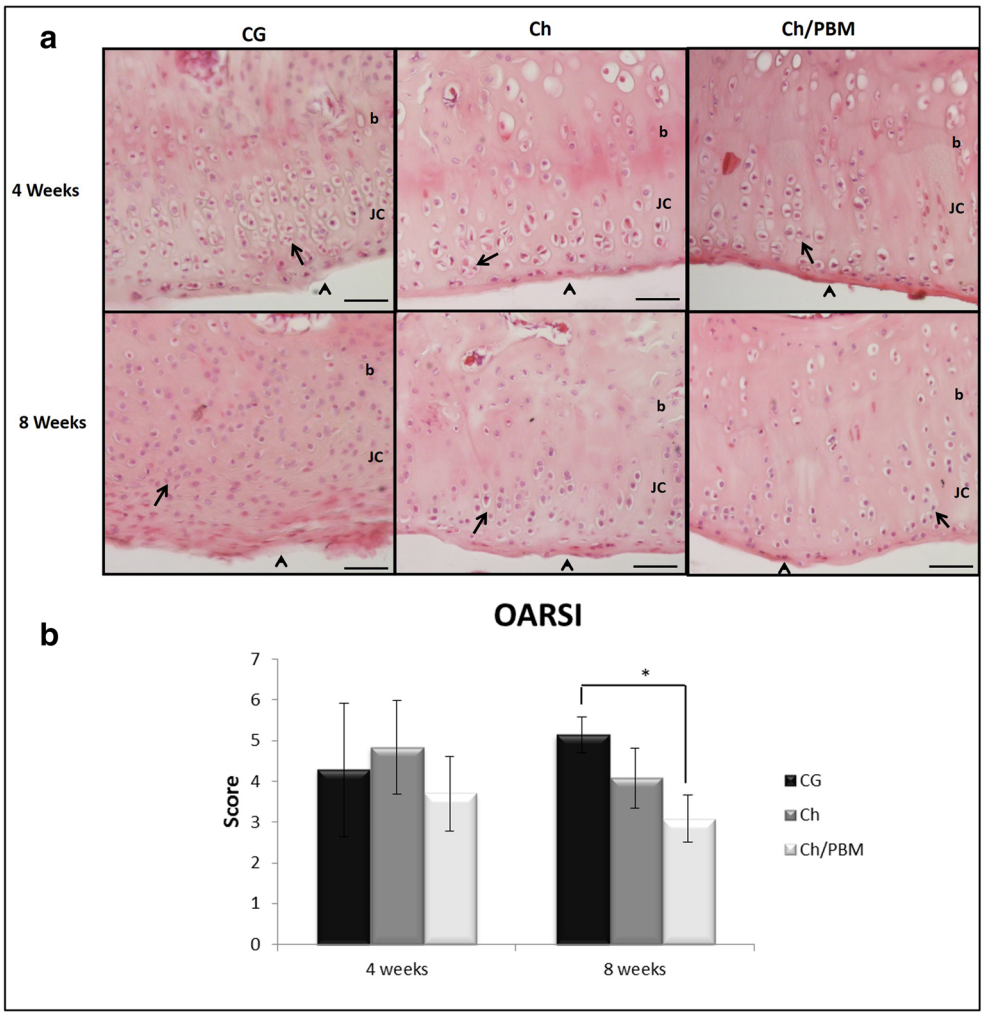

Fig. 3 **a** Histological descriptive analysis. Organization of chondrocytes (arrow), fibrillation and irregularities (arrowhead), joint cartilage (JC), subchondral bone (b). (Stain: HE; scale bar: 100 μm). **b** OARSI score system. Significant differences of $p < 0.05$ are represented by a single asterisk (*). CG, control group; Ch, chitosan group; Ch/PBM, chitosan and PBM group

TGF-β gene expression

The relative gene expression showed that Ch and Ch/PBM increase TGF-β expression compared with CG after 4 weeks. No other difference was observed between the treated groups after 8 weeks (Fig. 6b).

Discussion

This study aimed to investigate the in vitro and in vivo responses and cartilage repair potential of PBM associated with chitosan hydrogels. The main findings showed that it was possible to control the pH and hence the kinetics and degradation of chitosan hydrogels. The in vitro experiments showed that chondrocytes remained viable and proliferate on chitosan with or without PBM. In addition, in vivo experiments demonstrated the Ch/PBM and Ch produced a chondroprotective effect by modulate inflammation, stimulating as anabolic effectors, which can slow the progression of OA.

It is well known that PBM is able of decrease the level of cartilage damage and produce a better tissue structure, biomodulating the inflammatory process and reducing swelling. Moreover, chitosan can be used for different applications such as articular viscosupplementation, which is a intervention that proposes through an intra-articular injection of chitosan to deal with OA symptoms and to restore joint function (Pallotta et al. 2012). Thus, it was expected that the association of the viscosupplementation and PBM would culminate in an earlier resolution of the inflammatory process and reduce cartilage damage.

In order to explore the efficacy of chitosan as a potential viscosupplementation material in articular cartilage repair, a chitosan hydrogel with enzymatic control was used. Thus, this study showed that final pH values and gelation time of chitosan hydrogels were controlled by the concentration of urease and urea. These results corroborate with other studies that used pH-induced monolithic hydrogels which can be produced via uniform neutralization of slightly acidic chitosan solutions with ammonia generated from enzymatic hydrolysis of urea 30. Moreover, the literature shows that higher

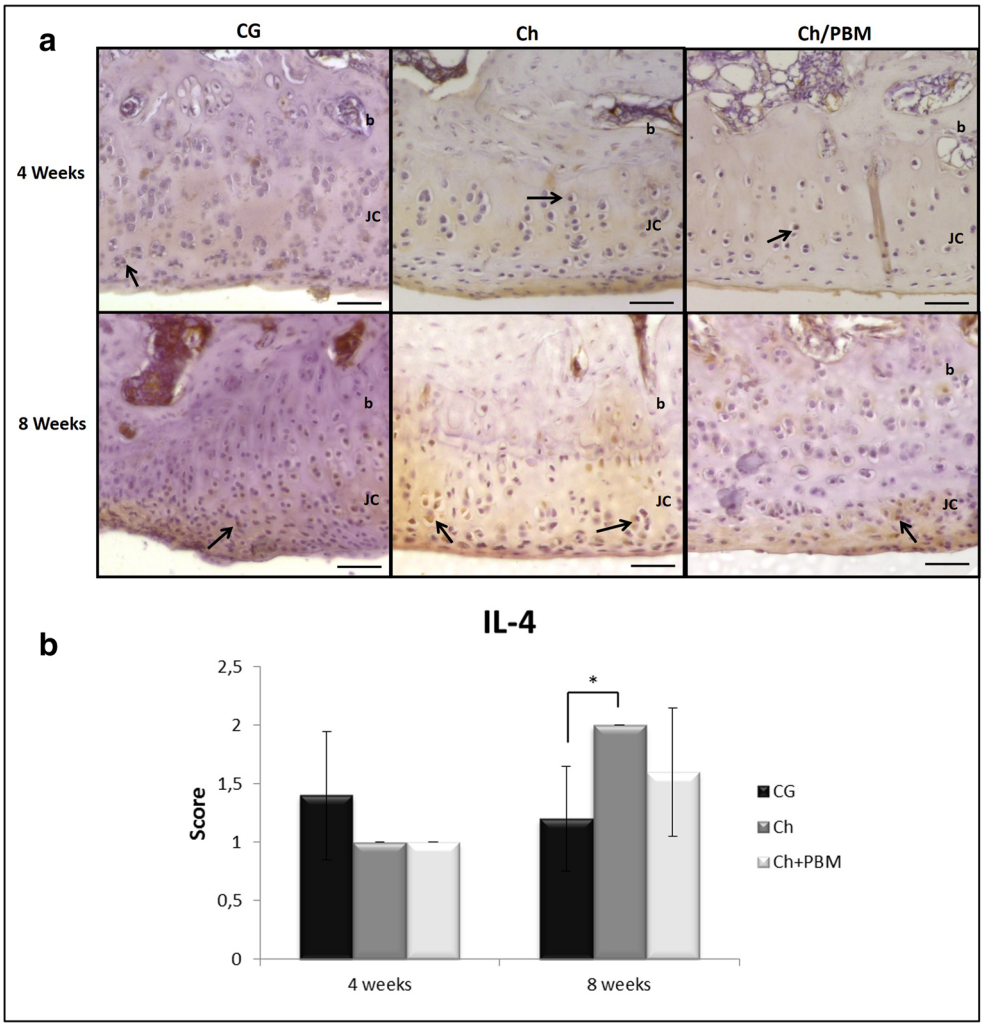

Fig. 4 **a** Immunohistochemistry analysis. Immunolabeled chondrocytes (arrow), joint cartilage (JC), subchondral bone (b). (scale bar: 100 μm). **b** Immunohistochemistry semi-quantitative analysis. Representative sections of IL-4 immunohistochemistry. Significant differences of $p < 0.05$ are represented by a single asterisk (*). CG, control group; Ch, chitosan group; Ch/PBM, chitosan and PBM group

concentrations of urea and urease resulted in faster pH increases and faster gelation (Assis et al. 2016; Yan et al. 2014b). The time gelation behavior is an important characteristic of the biomaterials that affects the hardening of the material and influences the handling of the injectable materials. This study demonstrated that time gelation of chitosan hydrogel was dependent of urea and urease concentrations. Similarly, other study observed that higher concentrations of

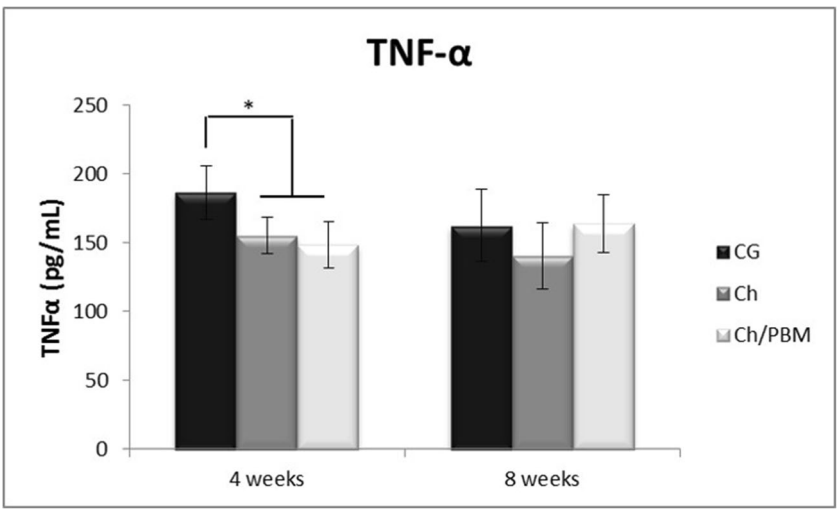

Fig. 5 TNF-α concentrations in synovial fluid of different groups by ELISA assays. Significant differences of $p < 0.05$ are represented by a single asterisk (*). CG, control group; Ch, chitosan group; Ch/PBM, chitosan and PBM group

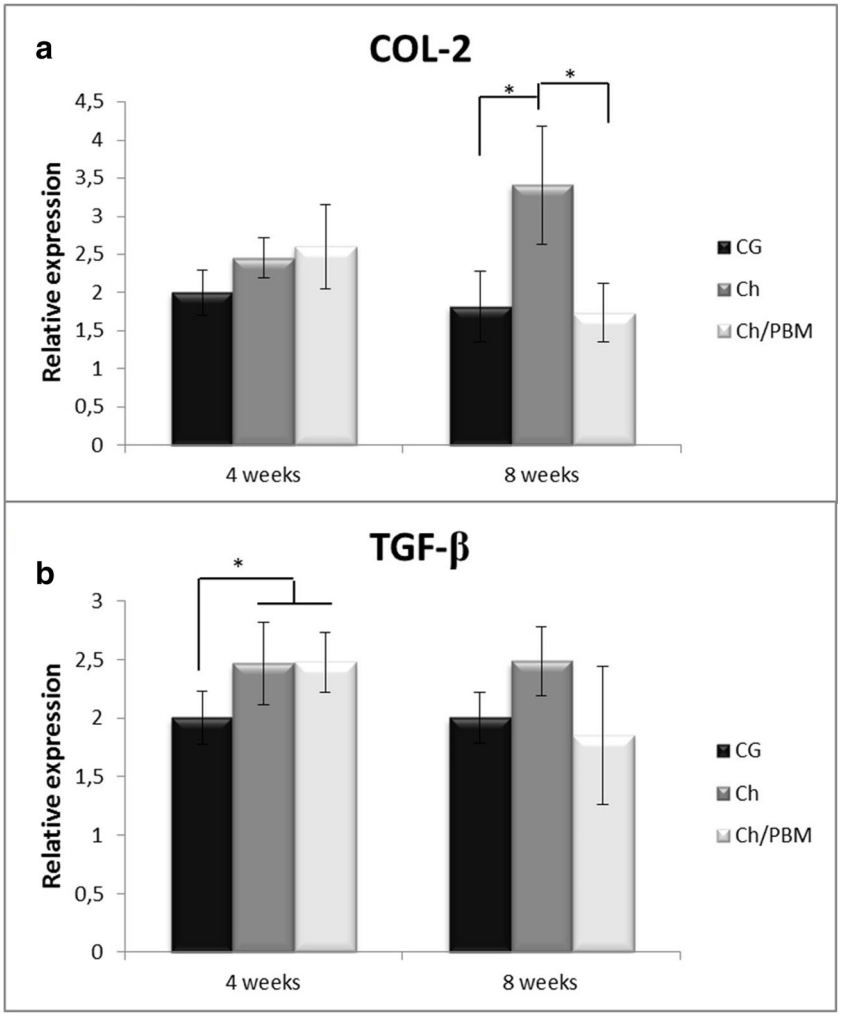

Fig. 6 Means and SD of the changes in the expression of the COL-2 and TGF-β genes by the RT-PCR. Significant differences of $p < 0.05$ are represented by a single asterisk (*). CG, control group; Ch, chitosan group; Ch/PBM, chitosan and PBM group

urease and urea caused hydrogel to have faster gelation (Wlodarczyk et al. 2018). In addition, the study findings showed that independent of urea and urease concentration, the chitosan hydrogels resulted in a remaining weight of up to 60% after soaking in lysozyme-containing PBS for 60 days. Our results corroborate those of Yan et al. (2014b) that show that degradation rates of chitosan at higher urease concentrations were faster degraded.

Additionally, it was evaluated the in vitro cellular response of PBM associated with chitosan hydrogel. In this study, cell metabolic activity showed that all CG were significantly higher compared with either Ch/PBM and Ch. However, all Ch/PBM and Ch groups presented that cell viability still reached 80% of that of the control. According to 33, cytotoxic effect is considered when reduction of cell viability by more than 30% occurs. Thus, these findings are supported by the many in vitro studies that have already demonstrated that chitosan is biocompatible and noncytotoxic (Yan et al. 2014b) (Sivashankari et al. 2017). For cell proliferation, Ch/PBM and Ch showed a DNA content peak on day 1, following with DNA content decrease in 3 and 5 days. Similarly, other studies showed that PBM and chitosan promoted the cell proliferation (Mighri et al. 2015; Wu et al. 2008).

Taken together, it is possible to suggest that these results could be related to the cell density. Confluence conditions in cell culture may interfere in replication and transcription, thus modifying the apoptotic response observed in confluent primary cells (Carvalho et al. 2003). Thus, the increased cell proliferation in Ch and Ch/PBM groups, on day 1, may have promoted cell confluence which culminated in cell apoptotic response. Thereby, it may explain the lower viability found in the Ch and Ch/PBM compared with the control group. On that way, it was showed that total number of cells and total cell density increased with time, but after that, the higher-density cultures expanded more slowly accompanied with high apoptosis levels (Song et al. 2009).

In addition, it is possible that PBM parameters used in this study promoted the dose–response, since it is well known that there are dose-dependent effects of PBM and the "Arndt–Schulz Law" is frequently quoted as a suitable model to describe the dose–response curve. Thus, weak stimuli slightly accelerate vital activity, stronger stimuli raise it further, but a

peak is reached and even stronger stimuli suppress it, until a negative response is finally achieved, which determines that stimulatory or inhibitory effects on biological tissues can be elicited depending on the amount of energy (Hamblin et al. 2011; Huang et al. 2009). In view of the aforementioned, it is possible to suggest that the energy from PBM, used in the in vitro analysis, was too high and may have overstimulated chondrocyte cells, preventing it to have a proliferation increase.

Furthermore, in this study, the qualitative histological and OARSI analyses showed similar findings in all groups in the first experimental period. However, on week 8, Ch/PBM was capable to attenuate OA modifications. It was recently demonstrated that chitosan may be used as a unique biological agent to prevent and treat osteoarthritis (Wu et al. 2008). It has been reported that PBM has a stimulatory effect on cartilage metabolism (Assis et al. 2016; Bublitz et al. 2014), which together with the chitosan ability to reduce the signs of synovitis might further influence in preventing cartilage degradation (Kunanusornchai et al. 2016).

Some cytokines, such as IL-4, has been demonstrated to have a chondroprotective effect, by regulating the anabolic effectors which can slow the progression of OA (Kunanusornchai et al. 2016). In the present study, immunohistochemistry analysis demonstrated an increased the IL-4 for Ch compared with other experimental groups after 8 weeks, indicating that this treatment had the ability to attenuate the progression of OA. In addition, it was demonstrated that IL-4 is a chondroprotective agent which inhibits IL-1β and TNF-a synthesis (Nordback et al. 2015).

It has been known that excess production of the inflammatory cytokines plays vital roles in the development of OA (Vincent et al. 2013). Among these cytokines, TNF-α has been shown to perform a pivotal role in OA as it contributes to cartilage matrix degradation (Heikkilä et al. 2017). TNF-α could activate inflammatory cells, which subsequently synthesize others pro-inflammatory chemokines to maintain inflammation in the development of OA (Mabey et al. 2016). Our findings demonstrated that Ch/PBM and Ch decreased TNF-α expression after 4 weeks, which may interfere in proteolytic pathways, exerting a protective effect against cartilage degradation in induced OA in rats. Some studies have demonstrated that PBM and Ch decreased pro-inflammatory cytokines such as prostaglandin E2, IL-1β, and TNF-α expression (Assis et al. 2016; Azuma et al. 2015; Guo et al. 2011).

Thus, it is possible to suggest that Ch was capable to modulate the inflammation by reducing catabolic (TNF-α) and stimulating anabolic cytokines (IL-4) which can result in a chondroprotective effect. As a result, the chondroprotective effect influenced the COL-2 expression observed in the Ch group after 8 weeks, possibly by the stimulation of chondrocyte activity, and prevented matrix degradation. It is well known that COL-2 is one of the main components of the extracellular matrix and it is markedly degraded with the progression of OA (Zhou et al. 2016). Moreover, several evidence have demonstrated that TGF-β favors the articular cartilage repair by stimulating events in chondrogenesis and the production of ECM proteins such as type II collagen and aggrecan (Finnson et al. 2012; Zhou et al. 2016). Thus, this study showed that Ch and Ch/PBM increased TGF-β expression compared with CG after 4 weeks. It is known that TGF-β plays an essential role in cartilage integrity and that it is a powerful tool to prevent or repair articular damage by counteracting the deleterious effects of pro-inflammatory cytokines (IL-1β and TNF-α) and inhibiting protease production (Davidson et al. 2007; Roman-Blas et al. 2007). Our results demonstrated that Ch and Ch/PBM could increase the gene related to components of the cartilage extracellular matrix, which can be related to the histological and immunohistochemistry analyses in the Ch and Ch/PBM groups. It was expected that the association of the viscosupplementation and PBM would culminate in a chondroprotective effect. However, the findings demonstrated that PBM was not effective in producing any extra stimulus to tissue for OA treatment. It is possible to suggest that these results could be related to the PBM parameters used in the present study. Although the effects of the PBM have been demonstrated by many authors, the regulatory mechanisms of PBM on tissues are poorly understood, especially when associated with a biomaterial. It may be due also to the redox potential of the target cells, which is associated with stimulation of cell function if it shifts toward oxidation and with inhibition if toward reduction. However, the reasons for the stimulatory and inhibitory effects of laser on cartilage repair remain unclear and warrant further investigation (Karu and Kolyakov 2005).

An important factor that should be considered in OA is the pain, which is the main symptom. Clinical trials have demonstrated that PBM has the ability to reduce swelling and pain and increase the functional activity in knee OA patients (Perrot 2015). Thus, PBM could be an effective therapeutic modality used for pain relief and improvement of function in patients with OA, mainly due to its ability to stimulate tissue metabolism, modulate the inflammatory process, and thus induce pain relief (Assis et al. 2016; Huang et al. 2015; Vassão et al. 2020).

In addition, it is known that the ends of the articulating bones are covered with a layer of smooth, whitish tissue, the articular cartilage. These bones move over one another, lubricated by synovial fluid, a product of the synovial lining of the joint. During movement, the synovial fluid acts as a lubricant and shock absorber, protecting the articular cartilage and joint structures from compressive and shear forces and thereby reducing articular cartilage wear. Also, it supplies oxygen and nutrients to the surrounding tissues and removes carbon dioxide and metabolic wastes. During osteoarthritis, synovial fluid becomes less viscous and inflammatory substances come into

direct contact with sensory nerve cells in the joint, producing the sensation of pain (Chakrabarti et al. 2020).

In view of this, the use of viscosupplementation, medical procedure during which a gel-like fluid is injected into the knee joint, has been used as part of the therapeutic arsenal in the conservative treatment of osteoarthritis of the knees (Hunter 2015; Strand et al. 2015). Thus, hyaluronic acid is currently used clinically as viscosupplements to relieve OA pain (Bannuru et al. 2011; Webb and Naidoo 2018). The viscoelastic properties of hyaluronic acid are directly related to molecular weight and concentration and are shear dependent. With slow movement and low shear, the linear chains of hyaluronic acid align slowly in the direction of the flow, and hyaluronic acid becomes more viscous, acting as a lubricant. In contrast, with faster impact, such as running or jumping, hyaluronic acid has inadequate time to re-align and has greater shock-absorbing properties. Thus, there is a need for more studies to investigate other materials that could be used in viscosupplementation (Henrotin et al. 2015).

There remains a need for robust scientific studies to help reduce the uncertainty around viscosupplementation and its role in a management strategy for OA. At the current time, the place of viscosupplementation in therapy and the decision as to which patient may be a candidate remain an individualized choice for discussion between the patient and treating physician.

This study was limited to a morphological protein and gene evaluation, information on the influence of Ch or Ch/PBM viscosupplementation on pain assessment. Also, it was performed on only one Ch application, thus it is required to investigate about the viscosupplementation injection frequency. Furthermore, there still is a need for additional high-quality, randomized control trials with placebos or comparators to clearly delineate the role of viscosupplementation in the treatment of pain in OA.

Conclusion

The results found in the present study indicate that the Ch and Ch/PBM prevented tissue degeneration by reducing catabolic and stimulating anabolic cytokines which can result in a chondroprotective effect. Therefore, these data highlight the potential of the association of PBM with Ch, to be used as a cartilage repair application.

Funding We thank the Brazilian funding agency FAPESP for the financial support of this research (FAPESP 2014/13702-6).

Compliance with ethical standards

Competing interests The authors declare that they have no competing interests.

Ethical approval This study was approved by the Ethics Committee on the Use of Animal under number 2478130315 and conducted according to the international norms of ethics on animal experimentation (National Research Council, 1996).

References

Assis L, et al. Aerobic exercise training and low-level laser therapy modulate inflammatory response and degenerative process in an experimental model of knee osteoarthritis in rats. Osteoarthr Cartil. 2016;24(1):169–77.

Azuma K, et al. Anticancer and anti-inflammatory properties of chitin and chitosan oligosaccharides. J Funct Biomater. 2015;6(1):33–49.

Bannuru RR, et al. Therapeutic trajectory following intra-articular hyaluronic acid injection in knee osteoarthritis-meta-analysis. Osteoarthr Cartil. 2011;19(6):611–9.

Bjordal JM, et al. The anti-inflammatory mechanism of low level laser therapy and its relevance for clinical use in physiotherapy. Phys Ther Rev. 2010;15(4):286–93.

Bublitz C, et al. Low-level laser therapy prevents degenerative morphological changes in an experimental model of anterior cruciate ligament transection in rats. Lasers Med Sci. 2014;29(5):1669–78.

Carvalho H, et al. Effect of cell confluence on ultraviolet light apoptotic responses in DNA repair deficient cells. Mutat Res Rev Mutat Res. 2003;544(2–3):159–66.

Chakrabarti S, et al. Human osteoarthritic synovial fluid increases excitability of mouse dorsal root ganglion sensory neurons: an *in-vitro* translational model to study arthritic pain. Rheumatology (Oxford). 2020;59(3):662–7.

Chen Z, et al. Novel chitosan hydrogel formed by ethylene glycol chitosan, 1, 6-diisocyanatohexan and polyethylene glycol-400 for tissue engineering scaffold: *in vitro* and *in vivo* evaluation. J Mater Sci Mater Med. 2014;25(8):1903–13.

Chung MJ, Park JK, Park Y. IL. Anti-inflammatory effects of low-molecular weight chitosan oligosaccharides in IgE–antigen complex-stimulated RBL-2H3 cells and asthma model mice. Int Immunopharmacol. 2012;12(2):453–9.

Comblain F, et al. Chitosan: a promising polymer for cartilage repair and viscosupplementation. Biomed Mater Eng. 2017;28(s1):S209–15.

Dantas MDM, et al. Improvement of dermal burn healing by combining sodium alginate/chitosan-based films and low level laser therapy. J Photochem Photobiol B Biol. 2011;105(1):51–9.

Davidson ENB, van der Kraan PM, van den Berg WB. TGF-β and osteoarthritis. Osteoarthr Cartil. 2007;15(6):597–604.

Finnson KW, et al. TGF-b signaling in cartilage homeostasis and osteoarthritis. Front Biosci (Schol Ed). 2012;4:251–68.

Galois L, et al. Dose–response relationship for exercise on severity of experimental osteoarthritis in rats: a pilot study. Osteoarthr Cartil. 2004;12(10):779–86.

Guo H, et al. Comparing different physical factors on serum TNF-α levels, chondrocyte apoptosis, caspase-3 and caspase-8 expression in osteoarthritis of the knee in rabbits. Joint Bone Spine. 2011;78(6):604–10.

Hamblin MR. Photobiomodulation or low-level laser therapy. J Biophotonics. 2016;9(11–12):1122–4.

Hamblin MR, et al. Biphasic dose response in low level light therapy-an update. Dose-Response. 2011;9(4):602–18.

Heikkilä HM, et al. The effect of intra-articular botulinum toxin A on substance P, prostaglandin E 2, and tumor necrosis factor alpha in the canine osteoarthritic joint. BMC Vet Res. 2017;13(1):74.

Henrotin Y, et al. Consensus statement on viscosupplementation with hyaluronic acid for the management of osteoarthritis. Semin Arthritis Rheum. 2015;45(2):140–9.

Huang YY, et al. Biphasic dose response in low level light therapy. Dose-Response. 2009;7(4):358–83.
Huang Z, et al. Effectiveness of low-level laser therapy in patients with knee osteoarthritis: a systematic review and meta-analysis. Osteoarthr Cartil. 2015;23(9):1437–44.
Hunter DJ. Viscosupplementation for osteoarthritis of the knee. N Engl J Med. 2015;372(11):1040–7.
Kaderli S, et al. A novel biocompatible hyaluronic acid–chitosan hybrid hydrogel for osteoarthrosis therapy. Int J Pharm. 2015;483(1–2):158–68.
Karu TI, Kolyakov SF. Exact action spectra for cellular responses relevant to phototherapy. Photomed Laser Surg. 2005;23(4):355–61.
Kunanusornchai W, et al. Chitosan oligosaccharide suppresses synovial inflammation via AMPK activation: an in vitro and *in vivo* study. Pharmacol Res. 2016;113:458–67.
Levinger I, et al. Increased inflammatory cytokine expression in the vastus lateralis of patients with knee osteoarthritis. Arthritis Rheum. 2011;63(5):1343–8.
Mabey T, et al. Plasma and synovial fluid inflammatory cytokine profiles in primary knee osteoarthritis. Biomarkers. 2016;21(7):639–44.
Mighri N, et al. Chitosan-coated collagen membranes promote chondrocyte adhesion, growth, and interleukin-6 secretion. Materials. 2015;8(11):7673–89.
Nordback PH, et al. Chitosan membranes in a rat model of full-thickness cutaneous wounds: healing and IL-4 levels. J Wound Care. 2015;24(6):245–51.
Pallotta RC, et al. Infrared (810-nm) low-level laser therapy on rat experimental knee inflammation. Lasers Med Sci. 2012;27(1):71–8.
Perrot S. Osteoarthritis pain. Best Pract Res Clin Rheumatol. 2015;29(1):90–7.
Rayegani SM, et al. Therapeutic effects of low level laser therapy (LLLT) in knee osteoarthritis, compared to therapeutic ultrasound. J Lasers Med Sci. 2012;3(2):71.
Rieger R, et al. Chitosan in viscosupplementation: in *vivo* effect on rabbit subchondral bone. BMC Musculoskelet Disord. 2017;18(1):350.
Roman-Blas JA, Stokes DG, Jimenez SA. Modulation of TGF-β signaling by proinflammatory cytokines in articular chondrocytes. Osteoarthr Cartil. 2007;15(12):1367–77.
Roos EM, et al. Muscle weakness, afferent sensory dysfunction and exercise in knee osteoarthritis. Nat Rev Rheumatol. 2011;7(1):57–63
Sanches M, et al. Chondroitin sulfate and glucosamine sulfate associated to photobiomodulation prevents degenerative morphological changes in an experimental model of osteoarthritis in rats. Lasers Med Sci. 2018;33(3):549–557.
Sivashankari PR, Moorthi A, Mohamed Abudhahir K, Prabaharan M. Preparation and characterization of three-dimensional scaffolds based on hydroxypropyl chitosan-graft-graphene oxide. Int J Biol Macromol. 2017;15(110):522–530.
Song IH, Caplan AI, Dennis JE. Dexamethasone inhibition of confluence-induced apoptosis in human mesenchymal stem cells. J Orthop Res. 2009;27(2):216–21.
Strand V, et al. Safety and efficacy of US-approved viscosupplements for knee osteoarthritis: a systematic review and meta-analysis of randomized, saline-controlled trials. J Pain Res. 2015;7(8):217–28.
van Houdt CIA, et al. Bone regeneration and gene expression in bone defects under healthy and osteoporotic bone conditions using two commercially available bone graft substitutes. Biomed Mater. 2015;10(3):035003.
Vassão PG, et al. Level of pain, muscle strength and posture: effects of PBM on an exercise program in women with knee osteoarthritis–a randomized controlled trial. Lasers Med Sci. 2020. https://doi.org/10.1007/s10103-020-02989-1
Vincent HK, et al. Hyaluronic acid (HA) viscosupplementation on synovial fluid inflammation in knee osteoarthritis: a pilot study. Open Orthop J. 2013;7:378.
Wang B, et al. Injectable nanohydroxyapatite-chitosan-gelatin microscaffolds induce regeneration of knee subchondral bone lesions. Sci Rep. 2017;7(1):16709.
Webb D, Naidoo P. Viscosupplementation for knee osteoarthritis: a focus on hylan G-F 20. Orthop Res Rev. 2018;10:73–81.
Wlodarczyk D, et al. Enzymatic gelation to prepare chitosan gels: study of gelation kinetics and identification of limiting parameters for controlled gel morphology. Int J Biol Macromol. 2018;107:1175–83.
Wu H, et al. Proliferation of chondrocytes on porous poly (DL-lactide)/chitosan scaffolds. Acta Biomater. 2008;4(1):76–87.
Yan X-Z, et al. Periodontal tissue regeneration using enzymatically solidified chitosan hydrogels with or without cell loading. Tissue Eng A. 2014a;21(5–6):1066–76.
Yan X, et al. Enzymatic control of chitosan gelation for delivery of periodontal ligament cells. Macromol Biosci. 2014b;14(7):1004–14.
Yurtkuran M, et al. Laser acupuncture in knee osteoarthritis: a double-blind, randomized controlled study. Photomed Laser Ther. 2007;25(1):14–20.
Zhang C, et al. The effects of chitosan oligosaccharides on OPG and RANKL expression in a rat osteoarthritis model. Acta Cir Bras. 2017;32(6):418–28.
Zhou S, et al. Influence of osteoarthritis grade on molecular signature of human cartilage. J Orthop Res. 2016;34(3):454–62.